First-principles calculations of molecular dissociation at surfaces [1]

D.M. Bird *, P.A. Gravil

School of Physics, University of Bath, Bath BA2 7AY, UK

Abstract

First-principles calculations, using a slab geometry and based on density functional theory, are having an increasing impact on our understanding of molecule–surface interactions. Calculations of molecular dissociation at metallic surfaces are briefly reviewed, and results are presented for the adsorption and dissociation of O_2 on Ag(110). It is shown that the calculated properties of the chemisorbed molecule agree well with experiment, but further from the surface there appears to be a significant over-binding, leading to inconsistencies with experiment.

Keywords: Chemisorption; Density functional calculations; Oxygen; Silver

1. Introduction

Consider one of the simplest examples of a molecule–surface reaction: a diatomic molecule in its ground state approaches a clean, unreconstructed metallic surface. The possible outcomes of this interaction include (i) reflection of the molecule back into the gas phase, (ii) sticking to the surface as an intact molecule, or (iii) dissociative adsorption. What would it take to calculate, from first principles, the relative probabilities of these alternatives? A moment's thought reveals what an immensely difficult problem this is, even for this apparently simple case. For a start, the final states of the reaction are not so straightforward; the reflected molecule may find itself in a variety of rotationally, vibrationally and electronically excited states, the molecularly adsorbed species might be in a number of possible adsorption geometries with different binding mechanisms (e.g. physisorption or chemisorption), and the mechanism by which the dissociated atoms lose their excess energy to the substrate might be crucial to the final state in dissociative adsorption. Coupled to this, for high accuracy, there is clearly a need for fully quantum mechanical calculations of the energetics and interatomic forces, which in principle requires solving the many-electron Schrödinger equation for an isolated molecule interacting with an effectively semi-infinite metallic substrate. Not an easy task!

Nevertheless, some very impressive progress has been made in recent years, and first-principles studies of the statics and dynamics of adsorption and dissociation have developed into a major field in surface science. The key approximations involved in current calculations are (i) the use of density functional theory to handle exchange and correlation effects, and (ii) the use of slabs or clusters to model the substrate. While density functional theory enables us to perform quantum

---

* Corresponding author.
[1] Invited paper.

mechanical calculations for rather large numbers of interacting atoms, it has the unfortunate effect of restricting calculations to ground-state properties. Non-adiabatic effects, including excitations of both substrate and molecule, are known to be of considerable importance in molecule–surface interactions [1]. The inclusion of excited states remains an important challenge for the future.

Three main approaches have been used to restrict the molecule–surface system to a manageable size. In some respects the most elegant is to use an embedding method, where the aim is to solve as accurately as possible for a small number of atoms around the adsorbate while taking the rest of the system into account through some form of embedding potential which acts like an additional boundary condition on the system. An example of this approach is given in Ref. [2], and while potentially very powerful, it has not yet developed as far as the methods outlined below. The second approach is to model the substrate as a finite cluster [3]. This is similar to the embedding approach, except that the effect of the rest of the substrate is neglected. The third technique involves the use of a supercell geometry, which has become popular largely because of its computational simplicity and efficiency. The semi-infinite substrate is replaced by a periodic array of extended, two-dimensional slabs, and the single adsorbate is also replaced by a periodic array. For example, Fig. 1 shows the supercell used for the calculations of O_2 adsorption on Ag(110) reported below. The question of whether supercells or clusters provide the more realistic representation of molecule–surface interactions remains a subject of some debate. In the limit of a very large number of atoms they must converge to the same result, but the rate of convergence need not be the same. To date, computational resources have not allowed a sufficiently detailed comparison of clusters and supercells to take place, because it is very expensive to increase the system size in either method to full convergence. This too remains an interesting project for the future.

Many calculations to date have focussed on H_2 dissociation, as this continues to provide an important testing ground for experimental and theoretical studies of gas–surface reactions [4–14]. A
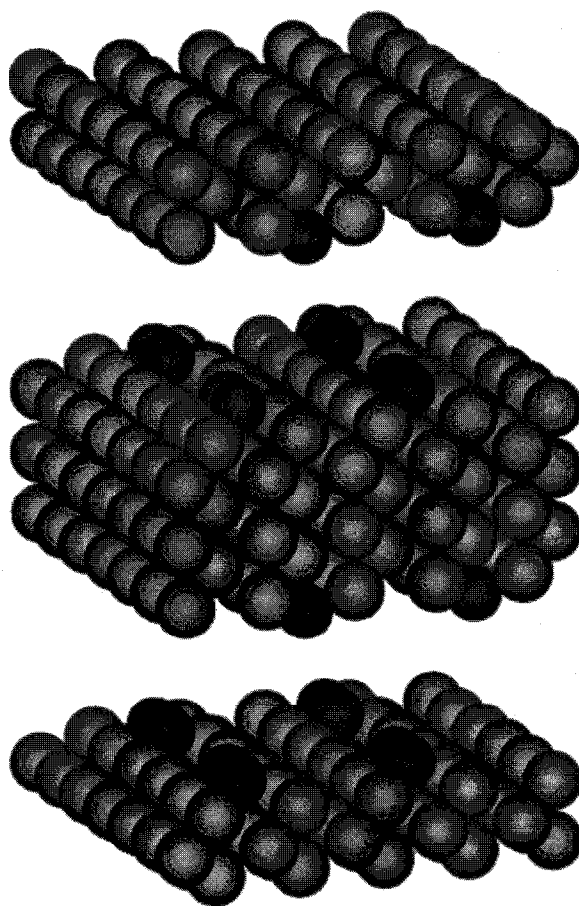

Fig. 1. The supercell used for calculations on O_2/Ag(110). Light and dark spheres represent Ag and O atoms, respectively. The O_2 molecules form a 3×2 supercell in the plane of the surface. The Ag slabs consist of six layers, and the gap between slabs is equivalent to a further six layers. With the theoretical GGA lattice parameter of 4.19 Å the supercell has dimensions of 8.89 Å × 8.38 Å × 17.78 Å.

number of important points have emerged from studies of H_2 dissociation which will strongly influence our approach to more complex gas–surface systems. First, it is clear that gradient-corrected density functionals (in particular, the generalised gradient approximation, GGA [15]) are crucial to obtain accurate energetics for molecule–surface systems; the familiar local density approximation (LDA) gives qualitatively as well as quantitatively incorrect results [5–7]. However, it remains an open question as to exactly how accurate the calculated potential energy surfaces

are, even when gradient corrections are employed, as it is very difficult to make a direct and detailed comparison between theory and experiment. Multidimensional dynamical simulations using ab-initio potential-energy surfaces have shown a good overall agreement with experiment, but several details are yet to be resolved [16–18]. Second, even close-packed surfaces appear significantly corrugated to an incoming molecule [6,7,11]. This corrugation is manifest, for example, in the variation of the magnitude of energy barriers over the surface and in the geometrical position of the barrier, and has important consequences for the dissociation dynamics [19]. Third, the strong variation of the potential energy both in translation over the surface cell and in molecular orientation leads to strong steering effects, which again strongly influence the dissociation dynamics, particularly at lower incident energies [14,16,20]. Finally, an analysis of the quantum states of the molecule–surface system has provided new insights into the electronic mechanism of H_2 dissociation [9,10,14].

All of these features can be anticipated to influence the modelling of adsorption and dissociation of heavier molecules, and there is now a clear interest in going beyond calculations on H_2 both to analyse systems of catalytic interest and to test whether current methods can be as successful as in the studies outlined above. Calculations on heavier molecules are, however, considerably more demanding for three main reasons. First, larger supercells are needed for larger molecules, and most current computational techniques scale as the cube of the number of atoms in the system. Second, it is important to consider the effects of substrate relaxation, which are neglected in all of the H_2 studies referred to above. Performing a full structural optimisation for each molecular configuration of interest is computationally very expensive, and a variety of test calculations are required to determine how important an effect relaxation has on the energetics. Third, several molecules of interest are spin-polarised (for example, O_2) and the inclusion of spin basically doubles the computational effort. Most work to date investigating heavier molecules has concentrated on looking at adsorbed species, rather than mapping out poten-

tial-energy surfaces for adsorption and dissociation. For example, a considerable amount of work has been carried out studying CO adsorption on a variety of surfaces using a supercell approach [21–23], and a review of related cluster calculations can be found in Ref. [3].

In the remainder of this paper we present results of calculations of the adsorption and dissociation of O_2 on Ag(110). Rather like the H_2–metal systems, O_2/Ag(110) can be regarded as a model system for adsorption and dissociation, as it has been very well characterised experimentally and dissociation is known to proceed via a mechanism involving sequential precursor states. We will show that when the O_2 molecule is close to the surface, our results are in good agreement with experiment. However, for larger molecule–surface separations we find inconsistencies with experiment due to an over-binding of the O_2 molecule. This is tentatively attributed to a failure of the GGA to provide sufficiently accurate energies, which, if confirmed, could have important consequences for future studies.

2. Adsorption and dissociation of O_2 on Ag(110)

The potential-energy surface (PES) for the O_2/Ag(110) system is characterised by three wells [24,25]: a molecular physisorbed state, a molecular chemisorbed state, and a dissociative (i.e. atomic) chemisorbed state. Transitions between these states can be thermally induced [25,26]. The physisorbed state, which is stable below 40 K, has the O_2 molecules lying down on the surface with the molecular axis along the $\langle 001 \rangle$ direction. The electronic structure of the molecule is essentially unchanged from that in the gas phase [25,27]. On warming the physisorbed state above 40 K, some molecules desorb while others convert to the chemisorbed phase. The molecule is strongly perturbed in this state, with a greatly extended bond length of around 1.47 Å and a greatly reduced vibrational quantum of 80 meV [28]. These compare to 1.21 Å and 190 meV, respectively, for the gas-phase molecule. The binding energy has been estimated as 0.4 eV [24], but because no ordered structure is formed the adsorption site and

orientation of the chemisorbed molecule remain a subject of some debate (see below). Above 150 K the O_2 molecules dissociate, and at higher temperatures a variety of ordered added-row reconstructions are formed [29]. In this paper we focus on two particular aspects of the adsorption and dissociation process, namely the structure of the chemisorbed state, and the entrance channel into this state from the gas-phase. Other features of our calculations are discussed elsewhere [30,31].

2.1. Orientation of the chemisorbed O_2 molecule

Most of our information about the structure of the chemisorbed state comes from near-edge X-ray absorption fine structure (NEXAFS) studies. Following the original work by Outka et al. [28], two high-resolution NEXAFS studies have been published [27,32]. Interestingly, these papers show spectra which are significantly different. The main features of the spectra taken at normal incidence are as follows. With the E-vector of the incident radiation along the $\langle 1\bar{1}0 \rangle$ orientation, both Guest et al. [27] and Pawela-Crew et al. [32] find a strong peak at around 533 eV. Although assignment of peaks is not certain, due to the strong perturbation of the O_2 molecule in the chemisorbed phase, the assignment of Ref. [28], that this peak arises the O 1s→σ_p^* transition, seems reasonable. The transition will be maximised when the polarisation vector lies parallel to the axis of the O_2 molecule, which supports the conventionally held view that the chemisorbed molecule has a $\langle 1\bar{1}0 \rangle$ orientation. However, with the polarisation vector in the $\langle 001 \rangle$ direction, Guest et al. [27] find a peak at about 534.5 eV which is absent in the spectra of Ref. [32]. Following the same assignment, that this is a σ_p^* peak, we conclude that this shows evidence of molecules with a $\langle 001 \rangle$ orientation. The two studies also differ in their preparation of the chemisorbed state. Guest et al. formed the state by warming to 50 K physisorbed molecules adsorbed at 25 K, while Pawela-Crew et al. dosed the surface with O_2 at 100 K, directly into the chemisorbed state. It would thus appear that different methods of preparation can lead to different populations of $\langle 1\bar{1}0 \rangle$- and $\langle 001 \rangle$-oriented molecules. First-principles calculations should be able to shed light on the relative stability of different molecular orientations, as well as on the favoured adsorption site, which in previous theoretical studies has been assumed to be at the long bridge [33,34].

2.2. Formation of the chemisorbed state

The relationship between the physisorbed, chemisorbed and dissociated states has been investigated by molecular beam methods [35,36]. Both studies find that the chemisorbed state acts as a precursor to dissociative chemisorption: no direct dissociation is observed for incident beam energies up to around 1 eV. Our first-principles calculations [31] show that the dissociation barrier from the chemisorbed state occurs at a very extended bond length (of the order of 2.2 Å), which is consistent with this experimental observation. Of more interest here is that adsorption is found to be activated and direct: the initial sticking probability falls markedly for molecules with incident kinetic energies below about 0.25 eV [35,36]. There is no upturn in sticking probability at very low incident energy, as is observed, for example, for O_2/Pt(111) [37,38]. This implies that the physisorbed state is *not* acting as a precursor for chemisorption for O_2/Ag(110), which at first sight is at variance with the thermally induced physisorbed-to-chemisorbed conversion discussed above. Heinzmann et al. [39] suggest that this apparent anomaly might be explained by a coverage-dependent effect. Again, first-principles calculations should help to resolve this question.

2.3. First-principles calculations

Our calculations are based on spin density functional theory and use a plane-wave, pseudopotential formalism. The total energy is minimised using an all-bands version of the conjugate-gradients method described in Refs. [11,40]. In performing spin-polarised calculations, the net polarisation is held at a fixed value of $2 \times \frac{1}{2}\hbar$ per molecule until the total energy is nearly converged, and is then allowed to relax to its ground-state value. Exchange and correlation effects are included within the Perdew–Wang form of the

GGA [15]. Our pseudopotential for Ag gives a lattice parameter of 4.19 Å and a bulk modulus of 85 GPa, which are in excellent agreement with other calculations [41,42]. The corresponding experimental values are 4.09 Å and 104 GPa, respectively. Calculations for the O_2 molecule give a binding energy, bond length and vibrational quantum of 5.5 eV, 1.24 Å and 0.18 eV, respectively. These are again in good agreement with previous calculations, and with the experimental values of 5.2 eV, 1.21 Å and 0.19 eV, respectively.

In order to separate the O_2 molecules as far as possible we use the large supercell shown in Fig. 1. A plan view of the 3×2 in-plane cell is shown in Fig. 2. In calculating the equilibrium adsorption structures, all atoms in the system are allowed to relax until the residual forces are less than 0.1 eV Å^{-1}. Details of the atomic displacements are given in Ref. [30]. Most calculations are performed with a plane-wave cut-off energy of 650 eV, and four k points in the surface Brillouin zone. A Fermi surface smearing of 0.25 eV is used, and the total energy extrapolated to zero temper-

ature. In order to check the convergence of our results, a number of representative geometries have been recalculated with nine k points in the Brillouin zone and a cut-off of 800 eV. The maximum change in energy is 0.05 eV, and the residual forces do not change significantly.

2.4. Results

The equilibrium adsorption structure has been calculated for four high-symmetry configurations with the O_2 molecule in the $\langle 1\bar{1}0 \rangle$ channels of the (110) surface (see Fig. 2). The calculated binding energy, bond length, adsorption height and O–O vibrational frequencies are given in Table 1. The results refer to a fully relaxed substrate and include spin-polarisation; the net polarisation is also shown in Table 1. Adsorption on top of the $\langle 1\bar{1}0 \rangle$ rows is unfavourable relative to the free molecule. In all cases the O_2 molecule prefers to lie flat on the surface. Table 1 shows that the favoured chemisorption site is the four-fold hollow, but also that there is no strong preference for either a $\langle 001 \rangle$ (A in Fig. 2) or a $\langle 1\bar{1}0 \rangle$ (B in Fig. 2) orientation. Indeed, within the expected accuracy of these calculations we cannot determine unequivocally which is the true ground-state. The binding energy and bond length of both species are in good agreement with experiment [24,28], but the calculated vibrational frequencies are rather higher than the experimental value of 80 meV [28]. In determining these frequencies, we have calculated the change in energy and force when the O–O bond is compressed and stretched about its equilibrium value, while holding the Ag substrate fixed. Also, only the harmonic part of the potential is considered. Both are likely to lead to an overestimate of the true vibrational frequency, so our calculated values are in reasonable agreement with experiment.

In order to estimate the barrier to transformation between species A and B in Fig. 2, we have calculated the energy for a molecule oriented between the two, at an angle of 45° to $[1\bar{1}0]$. This gives the barrier to rotation as 0.6 eV, but in this case the molecular axis has been forced to remain parallel to the surface, and so lower-energy pathways which involve a tilting of the molecule cannot be ruled out. Our results do, however, offer a
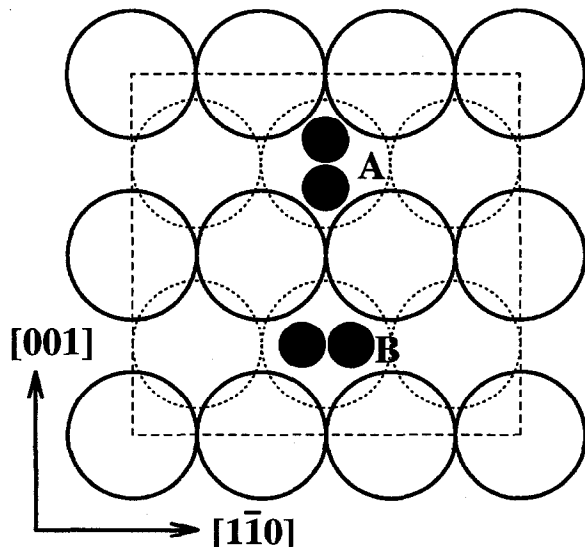

Fig. 2. Plan view of the Ag(110) surface. Full and dashed open circles denote top- and second-layer Ag atoms, respectively. The 3×2 supercell is marked by dashed lines. Filled circles represent O atoms. A and B refer to chemisorbed O_2 molecules in the four-fold hollow sites with molecular axes along [001] and $[1\bar{1}0]$, respectively.

Table 1
Calculated equilibrium properties of O_2 molecules adsorbed in high-symmetry sites of the Ag(110) surface

Site	Geometry axis[b]	Energy (eV)	Distance (Å)[c]		Polarisation[d] ($\frac{1}{2}\hbar$)	Frequency[e] (meV)
			O–O	O_2–Ag		
FFH[a]	$\langle 001 \rangle$	0.55	1.45	1.20	0.12	103
FFH	$\langle 1\bar{1}0 \rangle$	0.51	1.48	0.96	0.25	101
LB[a]	$\langle 001 \rangle$	0.37	1.32	2.07	1.23	119
LB	$\langle 1\bar{1}0 \rangle$	0.10	1.48	0.94	0.10	——

[a] FFH and LB refer to the four-fold hollow and long-bridge sites within the $\langle 1\bar{1}0 \rangle$ channels.
[b] This column gives the molecular orientation and the third the binding energy relative to separated slab and molecule.
[c] These columns give the O–O bond length and the height of the centre of the molecule above the top-layer Ag atoms, respectively.
[d] This column gives the net spin polarisation.
[e] This column gives the vibrational quantum of the O–O stretch vibration.

possible explanation of the NEXAFS results dis-
cussed above. It appears that in the study of Guest
et al. [27], both species A and B are present, while
Pawela-Crew et al. [32] find only B. The shorter
bond length we find for state A (see Table 1) is
consistent with the σ_p^* peak occurring at higher
energy, as found in Ref. [27]. The $\langle 001 \rangle$ orienta-
tion of the physisorbed molecule therefore seems
to promote a similarly oriented chemisorbed
species when the physisorbed-to-chemisorbed
transition is thermally induced. This species is not
present when molecules are absorbed directly into
the chemisorbed state, which could be either a
dynamical effect or due to the possibility that at
100 K (as in the experiments of Ref. [32]), the
rotational barrier between the two species is
overcome.

As discussed above, we have also calculated
pathways from the gas phase into the chemisorbed
state with the aim of investigating the interplay
between the physisorption and chemisorption wells
in the PES. The molecule is held above the
four-fold hollow site with its axis along $\langle 1\bar{1}0 \rangle$
(geometry B in Fig. 2), and has been moved away
from the surface to a height of about 3 Å. At all
points the O–O bond length and the Ag substrate
are allowed to relax, although for heights of greater
than 2 Å, Ag relaxation has a negligible effect on
the energy. The calculated binding energy is shown
in Fig. 3. As the molecule moves away from the
surface the bond length and spin polarisation also
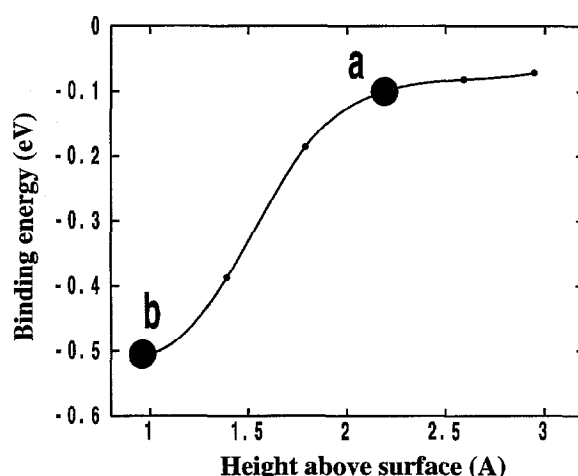return smoothly to their gas-phase values. The

Fig. 3. Calculated binding energy as a function of the height
of the O_2 molecule above the chemisorption site (four-fold
hollow with the molecular axis along $[1\bar{1}0]$). a and b show the
points corresponding to the bonding charge densities shown in
Figs. 4a and 4b, respectively.

change in the molecule–surface binding between
the points a and b in Fig. 3 is indicated in Fig. 4.
This shows isovalue surfaces of the bonding charge
density, $\delta\rho$, defined as

$$\delta\rho = \rho(O_2/Ag) - \rho(Ag\,slab) - \rho(O_2), \qquad (1)$$

where the ρ are the relevant charge densities. At
2.2 Å above the surface (Fig. 4a) there is a small
transfer of charge into the unoccupied π^* orbitals
of the O_2 molecule, with the largest transfer into
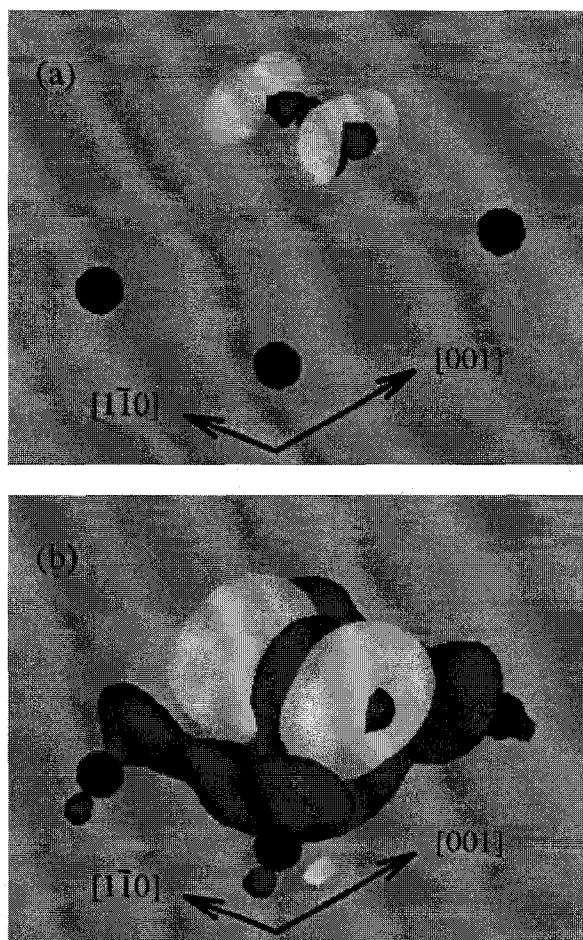the $\pi_{\parallel}^*$ orbital whose lobes lie parallel to the

Fig. 4. Iso surfaces of the bonding charge density for O_2 (a) 2.2 Å above the chemisorption site (four-fold hollow with the molecular axis along [1$\bar{1}$0]), and (b) in the equivalent chemisorption site. Light and dark contours enclose regions of positive and negative charge density, respectively. Black spheres denote the top-layer Ag atoms surrounding the four-fold hollow site.

surface. The total charge transfer at this point is about 0.28 electrons per O_2, and the net spin polarisation is equivalent to about 1.6 electrons (cf. 2 electrons for the gas-phase molecule). Even this far from the surface, then, we find a significant interaction. The charge transfer increases as the molecule moves closer to the chemisorbed state. In Fig. 4b we see that both $\pi_{\parallel}^*$ and $\pi_{\perp}^*$ are occupied; the net charge transfer is 0.80 electrons and the spin-polarisation is very small.

The most striking feature of Fig. 3 is that there is no energy barrier for entering the chemisorbed state from the gas phase. To analyse this further we have investigated a number of other geometries with the molecule 2.2 Å above the surface (as in Fig. 4a). Although there is some variation over the surface unit-cell, the general picture which emerges is that for molecules whose axes are parallel to the surface there is a binding between the molecule and the surface at this separation, and there is a force pulling the molecule closer to the surface (as in Fig. 3). This appears to be in conflict with molecular-beam studies, which indicate that adsorption into the chemisorbed state is activated [35,36]. The absence of a barrier in our calculations also rules out consideration of the way in which the physisorbed state acts as a precursor to chemisorption.

An analysis of the reasons for this difference between theory and experiment is currently under way. From checks on the quality of the pseudo-potentials used and convergence with respect to plane-wave cut-off and k-point sampling, we estimate that the calculated energies are accurate to within around 0.1 eV per O_2 molecule. This might then indicate that the over-binding we find for larger molecule–surface separations arises from the use of GGA functionals. This point clearly merits a much more detailed study, but a failure of the GGA to provide accurate energetics for this important molecule–surface reaction would have significant consequences for the reliability of other first-principles simulations.

Acknowledgements

References

[1] G.R. Darling and S. Holloway, Rep. Prog. Phys. 58 (1995) 1595.

[2] M.I. Trioni, G.P. Brivio, S. Crampin and J.E. Inglesfield, Phys. Rev. B 53 (1996) 8052.

[3] R.A. van Santen and M. Neurock, Catal. Rev., to be published.

[4] D.M. Bird, L.J. Clarke, M.C. Payne and I. Stich, Chem. Phys. Lett. 212 (1993) 518.

[5] B. Hammer, K.W. Jacobsen and J.K. Nørskov, Phys. Rev. Lett. 70 (1993) 3971.

[6] B. Hammer, M. Scheffler, K.W. Jacobsen and J.K. Norskov, Phys. Rev. Lett. 73 (1994) 1400.

[7] J.A. White, D.M. Bird, M.C. Payne and I. Stich, Phys. Rev. Lett. 73 (1994) 1404.

[8] G. Wiesenekker, G.J. Kroes and E.J. Baerends, J. Chem. Phys. 104 (1996) 7344.

[9] B. Hammer and J.K. Nørskov, Nature 376 (1995) 238.

[10] B. Hammer and J.K. Nørskov, Surf. Sci. 343 (1995) 211.

[11] J.A. White, D.M. Bird and M.C. Payne, Phys. Rev. B 53 (1996) 1667.

[12] S. Wilke and M. Scheffler, Phys. Rev. B 53 (1996) 4936.

[13] S. Wilke and M. Scheffler, Phys. Rev. Lett. 76 (1996) 3380.

[14] A. Eichler, G. Kresse and J. Hafner, Phys. Rev. Lett. 77 (1996) 1119.

[15] J.A. White and D.M. Bird, Phys. Rev. B 50 (1994) 4954.

[16] A. Gross, S. Wilke and M. Scheffler, Phys. Rev. Lett. 75 (1995) 2718.

[17] C.T. Rettner and D.J. Auerbach, Phys. Rev. Lett. 77 (1996) 404.

[18] A. Gross and M. Scheffler, Phys. Rev. Lett. 77 (1996) 405.

[19] G.R. Darling and S. Holloway, Surf. Sci. 304 (1994) L461.

[20] M. Kay, G.R. Darling, S. Holloway, J.A. White and D.M. Bird, Chem. Phys. Lett. 245 (1995) 311.

[21] B. Hammer, Y. Morikawa and J.K. Nørskov, Phys. Rev. Lett. 76 (1996) 2141.

[22] P. Hu, D.A. King, M.-H. Lee and M.C. Payne, Chem. Phys. Lett. 246 (1995) 73.

[23] P.H.T. Philipsen, G. te Velde and E.J. Baerends, Chem. Phys. Lett. 226 (1994) 583.

[24] C.T. Campbell, Surf. Sci. 157 (1985) 43.

[25] K.C. Prince, G. Paolucci and A.M. Bradshaw, Surf. Sci. 175 (1986) 101.

[26] Q.-S. Xin and X.-Y. Zhu, Surf. Sci. 347 (1996) 346.

[27] R.J. Guest et al., Surf. Sci. 278 (1992) 239.

[28] D.A. Outka et al., Phys. Rev. B 35 (1987) 4119.

[29] M. Canepa et al., Phys. Rev. B 47 (1993) 15823.

[30] P.A. Gravil, J.A. White and D.M. Bird, Surf. Sci. 352–354 (1996) 248.

[31] P.A. Gravil, D.M. Bird and J.A. White, to be published.

[32] J. Pawela-Crew, R.J. Madix and J. Stöhr, Surf. Sci. 339 (1995) 23.

[33] P.J. van den Hoek and E.J. Baerends, Surf. Sci. 221 (1989) L791.

[34] H. Nakatsuji and H. Nakai, J. Chem. Phys. 98 (1991) 2423.

[35] L. Vattuone, M. Rocca, C. Boragno and U. Valbusa, J. Chem. Phys. 101 (1994) 713.

[36] A. Raukema, D.A. Butler and A.W. Kleyn, J. Phys.: Condens. Matter 8 (1996) 2247.

[37] A.C. Luntz, M.D. Williams and D.S. Bethune, J. Chem. Phys. 89 (1988) 4381.

[38] C.T. Rettner and C.B. Mullins, J. Chem. Phys. 94 (1991) 1626.

[39] U. Heinzmann, S. Holloway, A.W. Kleyn, R.E. Palmer and K.J. Snowdon, J. Phys.: Condens. Matter 8 (1996) 3245.

[40] M.C. Payne et al., Rev. Mod. Phys. 64 (1992) 1045.

[41] A. Khein, D.J. Singh and C.J. Umrigar, Phys. Rev. B 51 (1995) 4105.

[42] B.D. Yu and M. Scheffler, Phys. Rev. Lett. 77 (1996) 1095.